Int. J. Heat Mass Transfer Vol. 21, pp. 1527–1542
Pergamon Press Ltd. 1978. Printed in Great Britain

A GENERALIZED CORRELATION OF CRITICAL HEAT FLUX FOR THE FORCED CONVECTION BOILING IN VERTICAL UNIFORMLY HEATED ROUND TUBES

Y. KATTO
Department of Mechanical Engineering, University of Tokyo,
Hongo, Bunkyo-ku, Tokyo, Japan

(*Received* 8 *February* 1978)

Abstract—The present study deals with the critical heat flux (CHF) in the conditions that the fluid fed to heated tubes is subcooled (including saturated liquid in the extreme situation) with no entrained vapor. To start with, postulating that there is a state where the hydrodynamic condition is responsible for CHF, a theoretical presumption for the generalized correlation equation of CHF is attempted with the aid of vectorial dimensional analysis. Then, the experimental data of CHF obtained from the literature for fluids of seven different kinds are analyzed, revealing the existence of four characteristic regimes of CHF, called L-, H-, N-, and HP-regime in this paper, and leading to the development of the generalized correlation of CHF data as well as that of CHF-regime correlation.

NOMENCLATURE

d, I.D. of heated tube [m];
G, mass velocity [kg/m²s];
H_{fg}, latent heat of evaporation [J/kg];
ΔH_i, enthalpy of inlet subcooling [J/kg];
K, parameter for the effect of inlet subcooling, equation (20);
l, length of heated tube [m];
p, absolute pressure, Figs. 5–14 and 16–18 [bar];
q_c, critical heat flux [W/m²];
q_{c0}, q_c, for $\Delta H_i = 0$ [W/m²];
u, inlet velocity [m/s].

Greek symbols

μ, viscosity [Ns/m²];
ρ_l, density of liquid [kg/m³];
ρ_v, density of vapor [kg/m³];
σ, surface tension [N/m];
χ_{ex}, exit quality.

1. INTRODUCTION

MANY studies have been made on the critical heat flux (CHF) or burnout for the forced convection boiling in vertical uniformly heated round tubes [1–4]. In the present paper, the discussion will be restricted to conditions where the fluid fed to the heated tube is subcooled with no entrained vapor (including the state of saturated liquid in the limit), and the flow is stable with no oscillations. Up to now, for such conditions as mentioned above, a lot of experimental data of CHF of water have been collected, and many empirical correlation for water have been developed by Tong *et al.* [5], Thompson and Macbeth [6], Bertoletti *et al.* [7], Tong [8], Hewitt *et al.* [9], Becker *et al.* [10], Bowring [11], and others. On the other hand, to make it possible to investigate CHF in nuclear reactors by employing model fluids such as Freons, the study of CHF modelling has been made by Barnett [12], Ahmad [13], etc., based on dimensionless analysis of the problem, and by Stevens and Kirby [14], Dix [15], etc., in pursuit of empirical scaling factors. Theoretical analyses of CHF have also been made by Whalley *et al.* [16], Thorgerson *et al.* [17], etc., evaluating the basic mechanisms of CHF. In addition, it should be noted that about twenty years ago, dimensional analyses of fundamental equations of two phase flow were made for the study of CHF independently by Zenkevich [18] and Griffith [19]. However, in spite of the effort mentioned above, the generalized correlation capable of predicting CHF for any arbitrary fluid, mass velocity, tube diameter and length has not yet been developed, and the present paper will report the result obtained in an attempt to derive a simple but dimensionless correlation of CHF.

2. A CLUE FOR ANALYZING DATA OF CHF

Considering only simple boiling systems of saturated liquid for the present, and postulating that the hydrodynamic condition of two-phase vapor–liquid flow is responsible for the occurrence of CHF, it may be assumed that the superficial vapor velocity $q_{c0}/\rho_v H_{fg}$ at the critical heat flux of q_{c0} is governed by the velocity of liquid u, the length of heated surface l, the densities ρ_l and ρ_v relating to the inertia, the surface tension of interface σ, the viscosities μ_l and μ_v relating to the viscous force, and the gravitational force $g(\rho_l-\rho_v)$ relating to the buoyancy. In this case, applying the dimensional analysis, it yields

$$\frac{q_{c0}}{\rho_v H_{fg} u} = f\left(\frac{\rho_l}{\rho_v}, \frac{\mu_l}{\mu_v}, \frac{\sigma}{\rho_l u^2 l}, \frac{\mu_l}{\rho_l u l}, \frac{g(\rho_l-\rho_v)l}{\rho_l u^2}\right). \quad (1)$$

If it is further assumed that the effect of viscous force

on CHF is negligibly small, equation (1) is simplified to

$$\frac{q_{c0}}{\rho_v H_{fg} u} = f\left(\frac{\rho_l}{\rho_v}, \frac{\sigma}{\rho_l u^2 l}, \frac{g(\rho_l-\rho_v)l}{\rho_l u^2}\right). \quad (2)$$

In the case of pool boiling, u can be eliminated from dimensionless groups in equation (2) to give

$$\frac{q_{c0}}{\rho_v H_{fg}} \Big/ \left[\frac{\sigma g(\rho_l-\rho_v)}{\rho_v}\right]^{1/4} = f\left[\frac{\rho_l}{\rho_v}, \frac{g(\rho_l-\rho_v)l^2}{\sigma}\right]. \quad (3)$$

As is well known, except the case of very small l (cf. [20]), the dimensionless group $g(\rho_l-\rho_v)l^2/\sigma$ in equation (3) has no effects on q_{c0}, when equation (3) agrees with the form of CHF correlation equation obtained by Zuber [21] or Kutateladze [22].

On the other hand, in the case of forced convection boiling, g can be eliminated from equation (2) to give immediately

$$\frac{q_{c0}}{\rho_v H_{fg} u} = f\left(\frac{\rho_l}{\rho_v}, \frac{\sigma}{\rho_l u^2 l}\right). \quad (4)$$

The form of equation (4) is in accord with those correlations obtained experimentally by Lienhard and Eichhorn [23] on heated cylinders in a cross flow, by Monde and Katto [24] on heated disks supplied with a liquid though a small impinging jet, and by Katto and Ishii [25] on rectangular heated surfaces supplied with a saturated liquid through a plane jet. For use afterward in the present paper, the above mentioned correlation of Katto and Ishii [25] is noted here as:

$$\frac{q_{c0}}{\rho_v H_{fg} u} = 0.0164\left(\frac{\rho_l}{\rho_v}\right)^{0.867}\left(\frac{\sigma}{\rho_l u^2 l}\right)^{1/3} \quad (5)$$

where u is the inlet velocity of liquid to the heated surface and l is the length of heated surface measured in the direction of forced flow.

Now, a more detailed analysis will be applied to equations (3) and (4) through the vectorial dimensional analysis. For the infinitesimal wave motion of an interface between the vapor and liquid flowing perpendicularly to gravity, such as illustrated in Fig. 1, the surface tension σ and the gravitational acceleration g exert their influence upon the fluid motion through changing the local pressure of fluid. Then, if Cartesian coordinates x, y, and z are taken as shown in Fig. 1, it is readily found from the well-known hydrodynamic theory of the wave motion [26] that σ and g should have

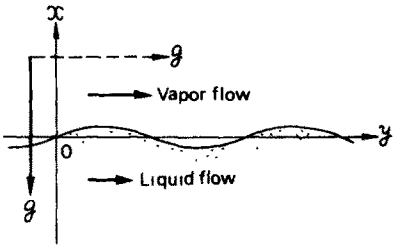

FIG. 1. Infinitesimal wave motion of a liquid–vapor interface.

the following dimensions:

$$[\sigma] = \frac{ML_y^2}{\theta^2 L_x L_z}, \quad [g] = \frac{L_y}{\theta^2} \quad (6)$$

where mass M, time θ, and length L (whose subscripts represent x, y, and z-axis respectively) are fundamental dimensions. In the meanwhile, if the direction of gravity is parallel to the liquid–vapor interface, as shown by a broken line of g in Fig. 1, g is independent of the wave motion so that it has the ordinary dimension $[g] = L_y/\theta^2$, which is the same as that given in equation (6). In other words, equation (6) can apply in either case of the direction of g mentioned above.

Figure 2(a) and (b) show the pool boiling on a horizontal and a vertical heated surface respectively. In both cases, however, equation (6) can equally apply to the liquid–vapor interface that is made very close to the heated surface by the vapor effusing perpendicularly from the heated surface, and besides, it is obvious that $[q_{c0}] = H/\theta L_x L_z$, $[H_{fg}] = H/M$, $[\rho] = M/L_x L_y L_z$ with the fundamental dimension of heat H, so that we obtain

$$\left[\frac{q_{c0}}{\rho_v H_{fg}}\right] = \frac{L_y}{\theta}, \left[\frac{\sigma g(\rho_l-\rho_v)}{\rho_v^2}\right] = \left(\frac{L_y}{\theta}\right)^4, \left[\frac{\rho_l}{\rho_v}\right] = 1. \quad (7)$$

The result of equation (7) means that equation (3) is truly dimensionless for both boiling systems of Fig. 2(a) and (b) provided the horizontal surfaces of extremely small size as well as the very long vertical surfaces are excluded.

Next, Fig. 2(c) shows the forced convection boiling where a liquid is fed to a heated surface of length l with the inlet velocity of u parallel to the heated surface. Taking into consideration that for the liquid–vapor interface that is made very close to the heated surface by the vapor effusing perpendicularly

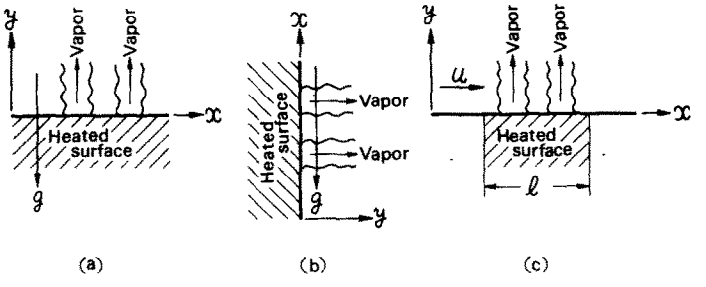

FIG. 2. Three kinds of fundamental boiling systems: (a) pool boiling on a horizontal surface, (b) pool boiling on a vertical surface, and (c) forced convection boiling on a flat surface.

from the heated surface, σ has the dimension given in equation (6), and $[q_{c0}] = H/\theta L_x L_z$, $[H_{fg}] = H/M$, $[\rho] = M/L_x L_y L_z$, $[u] = L_x/\theta$, and $[l] = L_x$, it yields readily

$$\left[\frac{q_{c0}}{\rho_v H_{fg} u}\right] = \frac{L_y}{L_x}, \left[\frac{\rho_l}{\rho_v}\right] = 1, \quad \left[\frac{\sigma}{\rho_l u^2 l}\right] = \left(\frac{L_y}{L_x}\right)^3. \quad (8)$$

The result of equation (8) means that in order for equation (4) to be truly dimensionless, it should take the form of $q_{c0}/\rho_v H_{fg} u = f(\rho_l/\rho_v)(\sigma/\rho_l u^2 l)^{1/3}$, which is nothing but the form of those correlations experimentally obtained in [24] and [25], such as that given in equation (5). As for the correlation obtained by Lienhard and Eichhorn [23], which has a slightly different form from above, it should be noted that the vectorial conditions of this boiling system are not so simple as that of Fig. 2(c).

The above results, given for Fig. 2(a), (b) and (c), may be regarded to show that the vectorial dimensional analysis is not useless for the analysis of CHF in the case of simple boiling systems at least.

Now, let us consider a uniformly heated round tube of internal diameter d and heated length l, to which a saturated liquid with no entrained vapor is

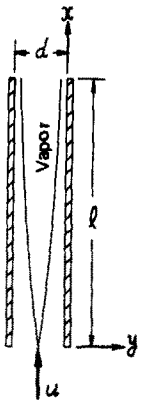

FIG. 3. A uniformly heated tube in the limit as $d \to 0$.

fed with the inlet velocity u. In this case, if the limit as $d \to \infty$ is assumed, the hydrodynamic state is the same as that of Fig. 2(c), so that there is a possibility of obtaining a correlation of CHF similar to equation (5). On the other hand, for the limit as $d \to 0$, it may be presumed that due to the accumulation of vapor in the tube, CHF occurs in such the state as illustrated in Fig. 3, and the liquid–vapor interface parallel to the heated surface is responsible for the occurrence of CHF; for which the vectorical dimensional analysis yields

$$\left[\frac{q_{c0}}{\rho_v H_{fg} u}\right] = \frac{L_y}{L_x}, \text{ and } \left[\frac{\sigma}{\rho_l u^2 l}\right] = 1. \quad (9)$$

In this case, therefore, the truly dimensionless correlation is assumed to take the following form:

$$\frac{q_{c0}}{\rho_v H_{fg} u} \cdot \frac{l}{d} = \text{const.} \left(\frac{\rho_l}{\rho_v}\right)^a \left(\frac{\sigma}{\rho_l u^2 l}\right)^b. \quad (10)$$

It is of interest to note that the LHS term of equation (10) multiplied by ρ_v/ρ_l is a quantity proportional to the quality χ_{ex} at the tube exit. Then, trying to invent those correlations which take the form of equation (5) as $d \to \infty$ and that of equation (10) as $d \to 0$, the following equation is found to be one of the equations satisfying the above conditions:

$$\frac{q_{c0}}{GH_{fg}} = \text{const.} \left(\frac{\rho_v}{\rho_l}\right)^{0.133} \left(\frac{\sigma\rho_l}{G^2 l}\right)^{1/3} \times \frac{1}{1 + \text{const.} \left(\frac{\rho_l}{\rho_v}\right)^m \left(\frac{\sigma\rho_l}{G^2 l}\right)^n \frac{l}{d}} \quad (11)$$

where $G = \rho_l u$, that indicates the mass velocity through the tube because of the premise that saturated liquid is fed to the tube with the velocity of u.

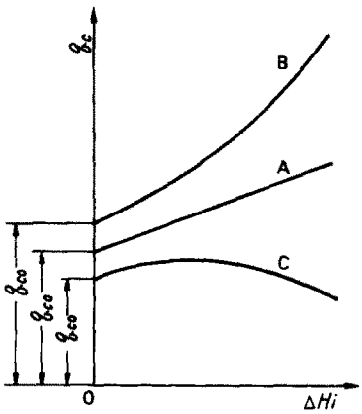

FIG. 4. Relationship between q_c and ΔH_i (type A found in L-, H-, and HP-regime; type B in N-regime, and type C in VL-regime).

3. ANALYSIS OF q_{c0}-DATA (H-REGIME)

In order to test the validity of equation (11), an analysis is attempted by using the esperimental data of q_{c0} which can be obtained in the following way. When the inlet subcooling ΔH_i changes in an experiment keeping the other conditions constant, the relationship between the critical heat flux q_c and the inlet subcooling enthalpy ΔH_i is linear in many cases as illustrated by type A in Fig. 4 but occasionally has the curvature such as illustrated by type B or C in Fig. 4 depending on the conditions. In any case, however, if there are enough data of $q_c - \Delta H_i$ to permit the extrapolation as $\Delta H_i \to 0$, q_{c0} can be determined with accuracy. In the present analysis, q_{c0} is thus determined from the data compiled or presented by Thomson and Macbeth (Tables 1–10) [6], Becker *et al.* (data of inlet subcooling 10°C in Fig. 12) [10], Waters *et al.* [27], Lowdermilk *et al.* (Table IV) [28], Chojnowski and Wilson (Fig. 3) [29], Lee and Obertelli [30], Matzner [31], Weatherhead [32], Barnett [33] and Hewitt *et al.* (Fig. 2.8) [34] for water; Stevens *et al.* [35, 36] for Freon-12; Dix (CHF $\times 10^{-4}$ should be replaced by CHF $\times 10^{-5}$ in Tables of Appendix) [15]

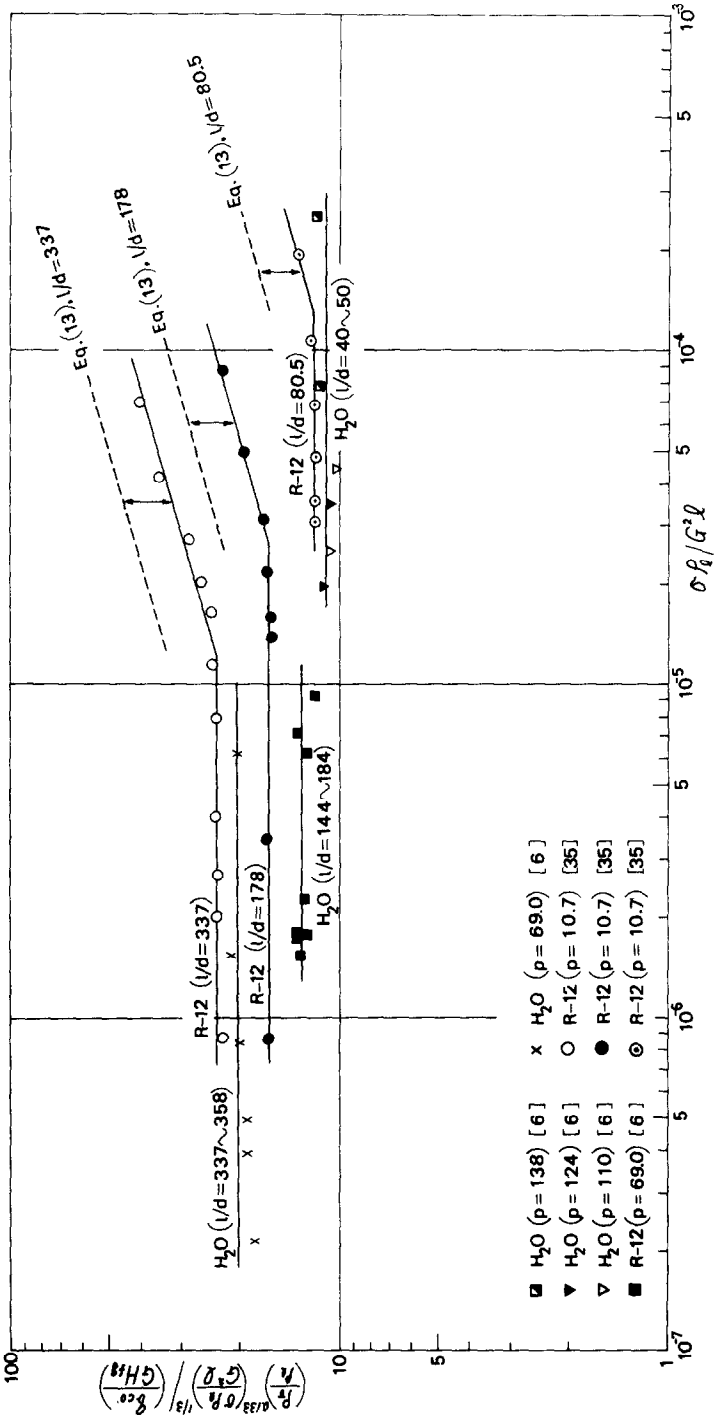

FIG. 5. Characteristics of q_{c0} in H-regime.

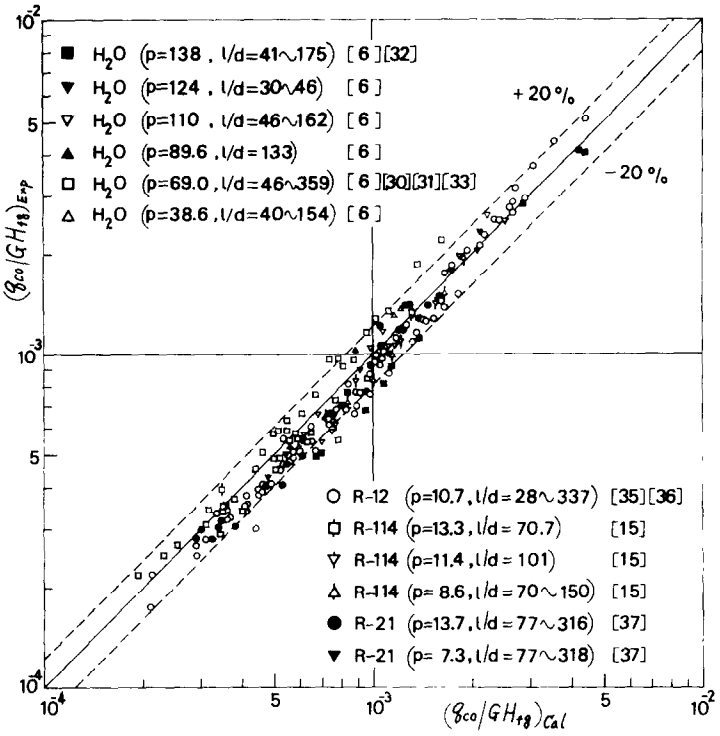

FIG. 6. Comparison of the prediction of equation (12) with the experimental data in H-regime.

for Freon-114; Barnett and Wood [37] for Freon-21; Lewis *et al.* [38] for liquid hydrogen and nitrogen; and Ogata and Sato [39] for liquid helium.

Now, Fig. 5 shows some typical results obtained in the region of $\sigma\rho_l/G^2l = 10^{-7}$ to 10^{-3}, indicating that there is a regime where the value of ordinate is determined as a function of l/d alone independently of the change of $\sigma\rho_l/G^2l$; and the data of q_{c0} belonging to this regime can be correlated fairly well by the following dimensionless equation:

$$\frac{q_{c0}}{GH_{fg}} = 0.10\left(\frac{\rho_v}{\rho_l}\right)^{0.133}\left(\frac{\sigma\rho_l}{G^2l}\right)^{1/3}\frac{1}{1+0.0031\,l/d}. \tag{12}$$

In Fig. 6, all the experimental data of q_{c0}/GH_{fg} in this regime got from the data source cited before are compared with the prediction of equation (12).

Probably, it may be presumed that CHF in this regime is affected by the hydrodynamic instability conditions akin to those assumed in deriving equation (11). Accordingly, this regime will be called H-regime in this paper. As for the effect of inlet subcooling on CHF, the details of which will be described in Chapter 6, such a linear relationship as shown by the type A in Fig. 4 is found to be always established between q_c and ΔH_i in H-regime.

4. ANALYSIS OF q_{c0}-DATA (OTHER REGIMES)

4.1. *L-regime*

Figure 7 as well as a part of Fig. 5 shows typical results obtained in the region of $\sigma\rho_l/G^2l$ relatively higher than that of H-regime; and the data of q_{c0} belonging to this regime can be correlated fairly well by the following dimensionless equation:

$$\frac{q_{c0}}{GH_{fg}} = 0.25\left(\frac{\sigma\rho_l}{G^2l}\right)^{0.043}\frac{1}{l/d} \tag{13}$$

except Freons for which, as shown by broken lines in Fig. 5, equation (13) gives the prediction of q_{c0} higher than the experimental data as much as about 1.36 times, so that the constant of 0.25 in equation (13) must be replaced by 0.34. The reason for this is unknown, but it may depend on the thermal decomposition of Freons on the dried heated surface. In Fig. 8, all the experimental data of q_{c0}/GH_{fg} in this regime which are obtained from the data sources cited in Chapter 3 are compared with the prediction of equation (13) (with the constant as 0.34 for Freons).

It can be presumed that the dryout of an annular liquid-film flowing over the tube wall is mainly responsible for CHF in this regime; because the main part of equation (13) excluding the term of very weak effect of $\sigma\rho_l/G^2l$, that is $q_{c0}/GH_{fg} = 0.25/(l/d)$, is nothing but the condition corresponding to the complete exhaustion of liquid at the exit of the tube with the uniform heat flux of q_{c0}.

Since this regime has the mass velocity G less than that in H-regime, it is called L-regime in this paper. As for the effects of inlet subcooling, a linear relationship is found to be established between q_c and ΔH_i in L-regime (that is, the type A in Fig. 4).

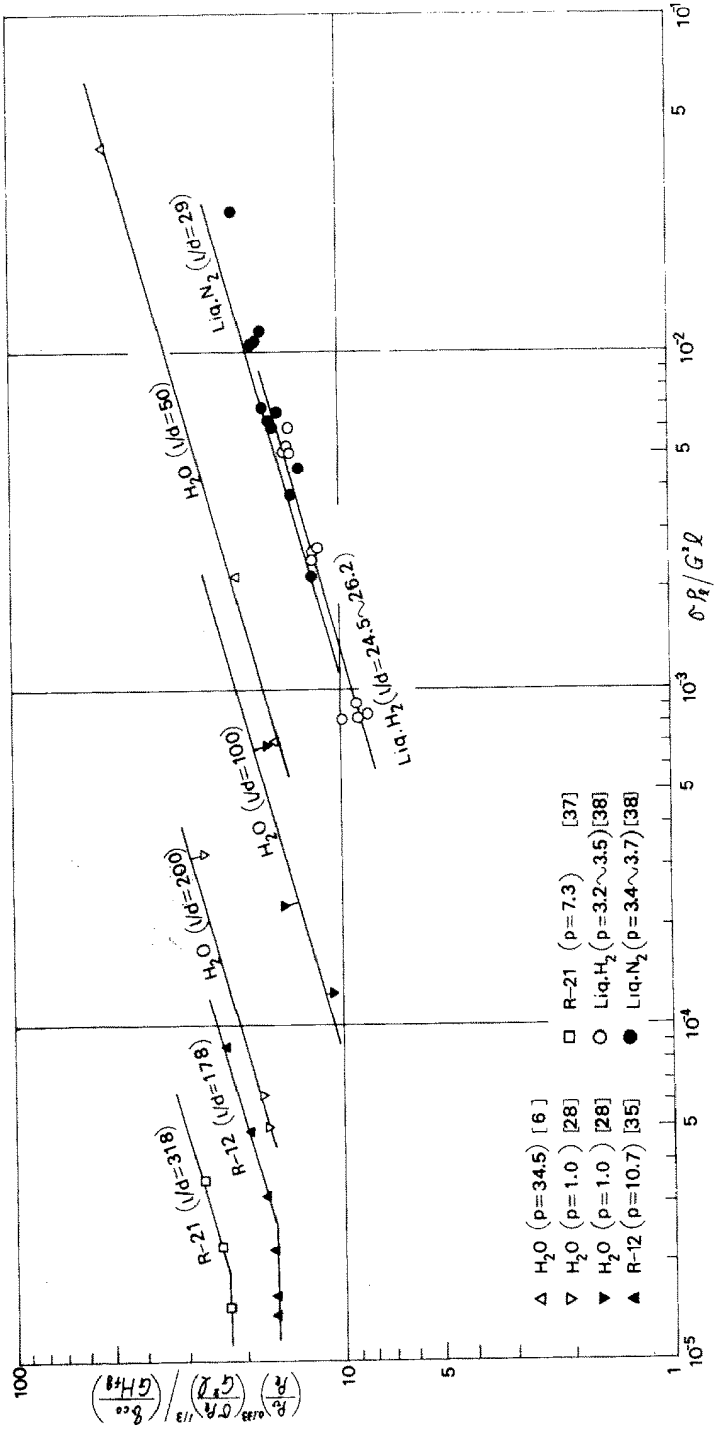

FIG. 7. Characteristics of q_{c0} in L-regime.

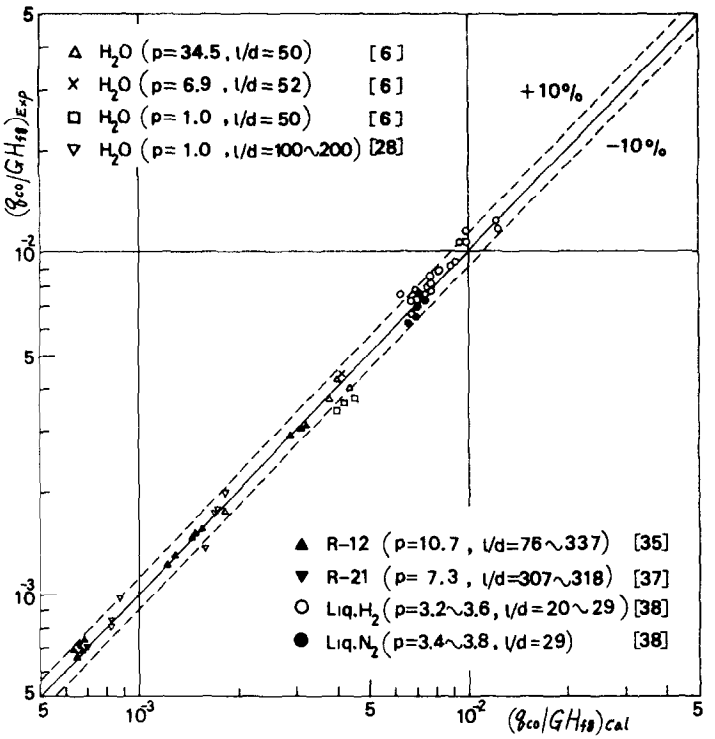

FIG. 8. Comparison of the prediction of equation (13) with the experimental data in L-regime.

Supplementary note: VL-regime. When the mass velocity G is further reduced to low levels so that the inlet velocity of liquid is less than, say, 0.2–0.3 m/s, and when the length of tube is considerably short, there is a possibility of bringing about the deviation from L-regime toward the regime where ordinary pool boiling exerts its influence on CHF. Figure 9 shows two examples of the deviation from L-regime found in the existing experimental data. Because of the very low mass velocity, this regime is called VL-regime in this paper. It should be stressed that when the liquid fed to the tube is subcooled, the non-linear relationship of type C in Fig. 4 appears in VL-regime.

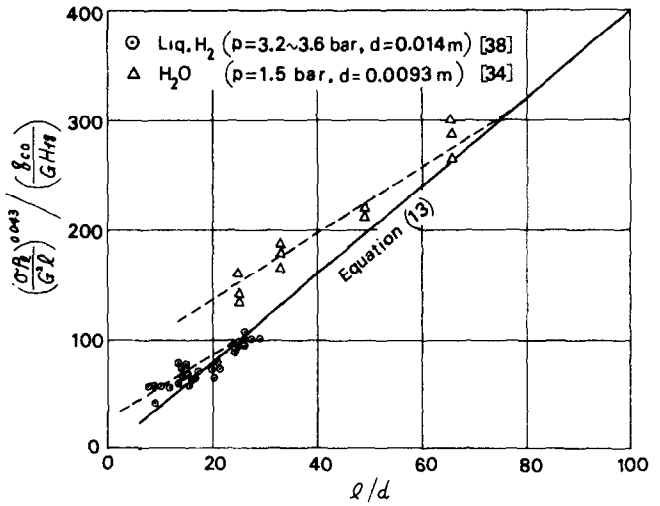

FIG. 9. Deviation from equation (13) in VL-regime.

4.2. *N-regime*

As shown in Fig. 10, when $\sigma\rho_l/G^2l$ is reduced from the state of H-regime keeping l/d constant, the value of ordinate tends to increase entering a new region indicated by black symbols of data, where the non-linear relationship of type B in Fig. 4 is found to appear. The data of q_{c0} in this regime can be correlated by the following dimensionless equation:

$$\frac{q_{c0}}{GH_{fg}} = 0.098\left(\frac{\rho_v}{\rho_l}\right)^{0.133}\left(\frac{\sigma\rho_l}{G^2l}\right)^{0.433}\frac{(l/d)^{0.27}}{1+0.0031\,l/d}. \tag{14}$$

Figure 11 shows the comparison of equation (14) with all the experimental data of q_{c0} in this regime, the

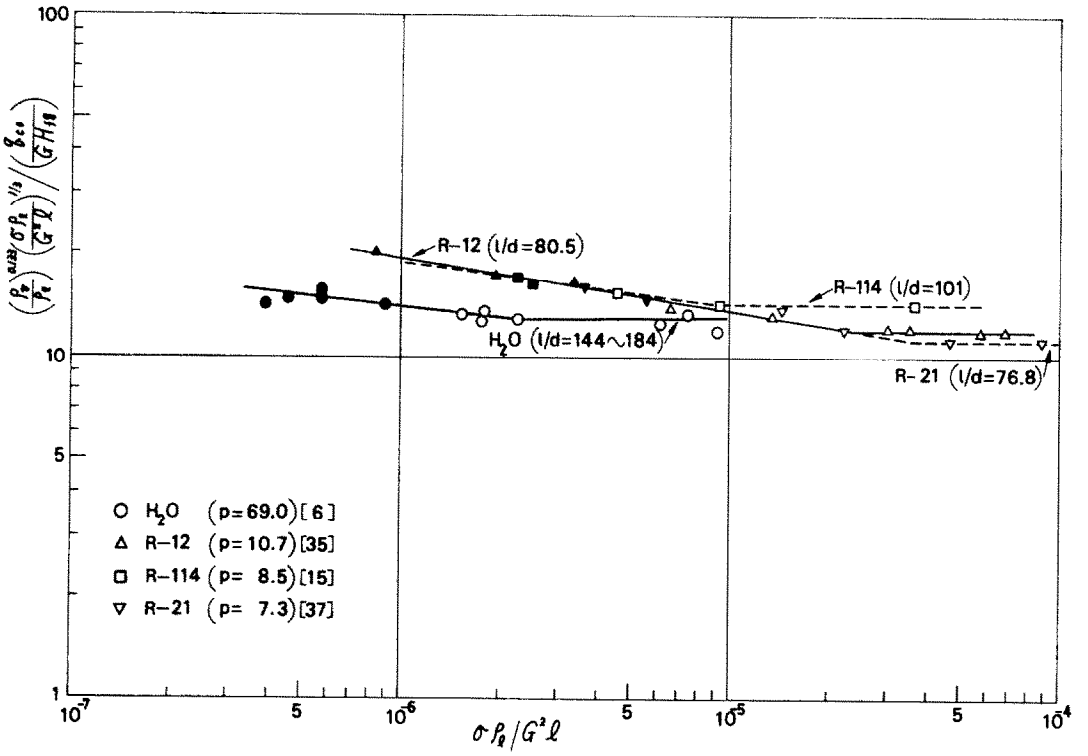

FIG. 10. Characteristics of q_{c0} in N-regime.

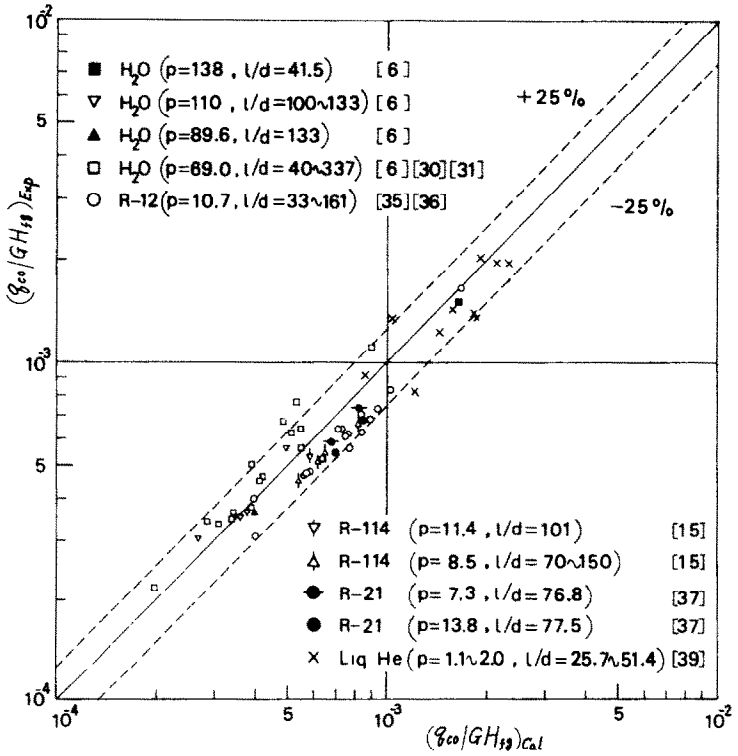

FIG. 11. Comparison of the prediction of equation (14) with the experimental data in N-regime.

error being a little greater than those in other regimes.

This regime is characterized by the non-linear relationship of type B in Fig. 4 between q_c and ΔH_i, so that it is called N-regime in this paper. Generally CHF takes place in this regime with low exit quality in the neighborhood of zero, and accordingly it may be presumed that a bubble layer flows parallel to the tube wall with a liquid core flowing at the center of the tube when CHF appears due to the transition to the film boiling.

Such transitional data as those shown by blank, that is non-black, symbols lying in slant lines in Fig. 10 can be correlated by equation (14), but they are

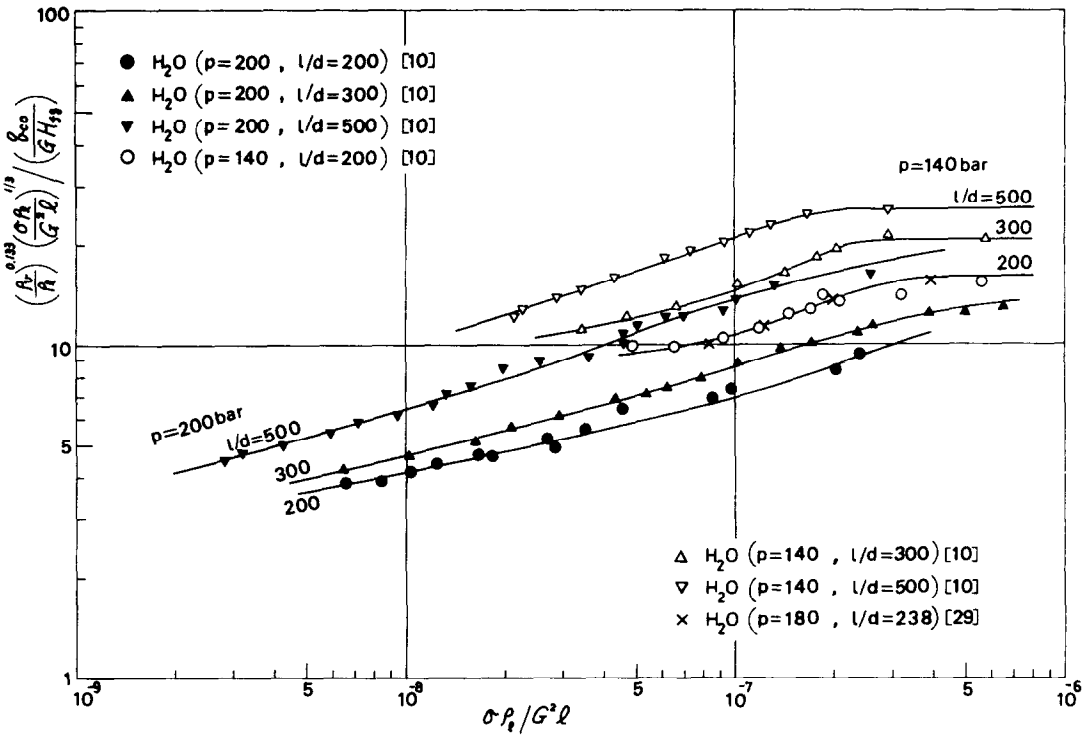

FIG. 12. Characteristics of q_{c0} in HP-regime.

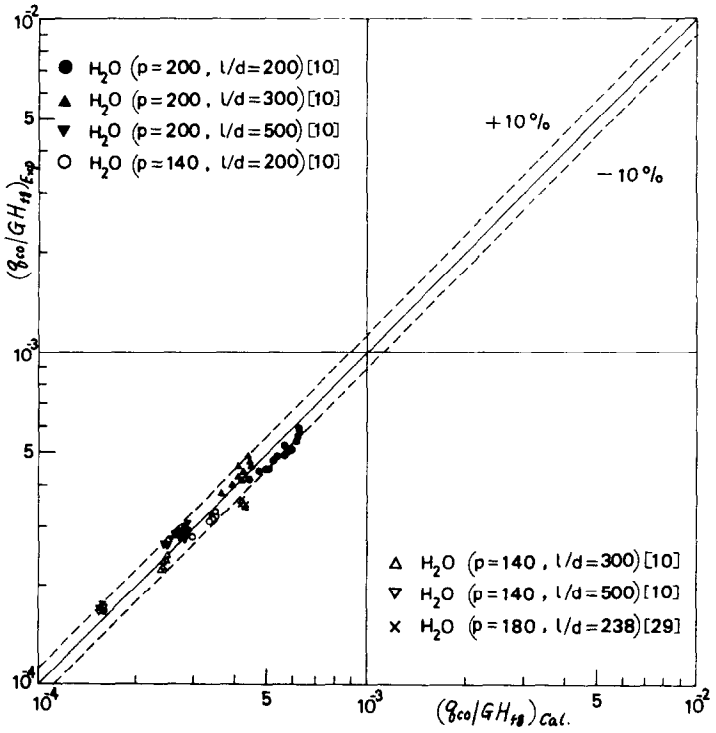

FIG. 13. Comparison of the prediction of equation (15) with the experimental data in HP-regime.

regarded as belonging to H-regime in the point that the linear relationship is established between q_c and ΔH_i. Accordingly, in the present paper, they have been correlated by equation (12) of H-regime in order to avoid the complexity.

4.3. *HP-regime*

In the region of $\sigma\rho_l/G^2l$ less than that of H-regime, it is found that there is another regime where the linear relationship is established between q_c and ΔH_i, and at the same time, such characteristics as shown

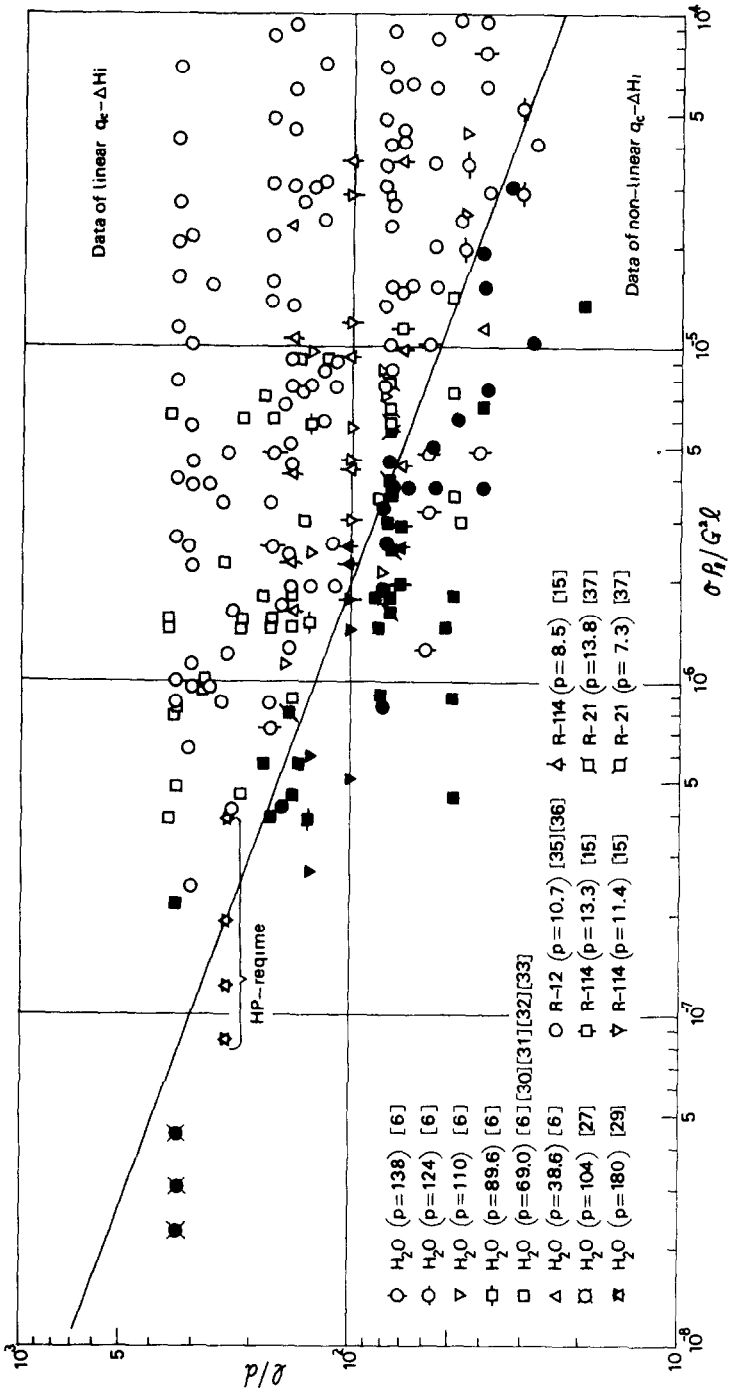

FIG. 14. Boundary between H-regime and N-regime.

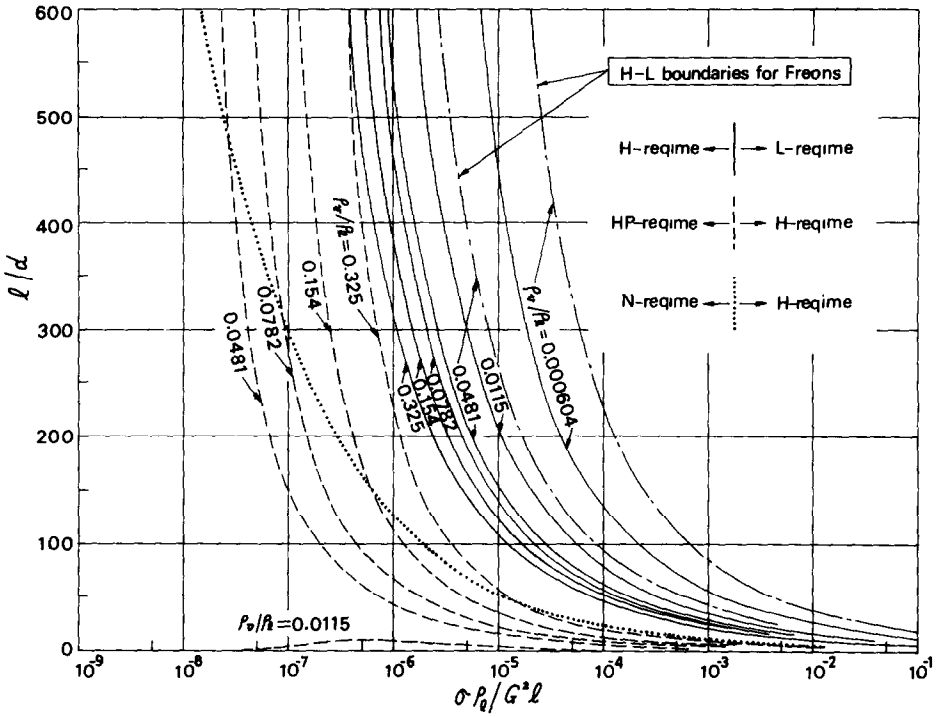

FIG. 15. CHF-regime map.

in Fig. 12 appear for CHF. The data of water only have been obtained in this regime, but they can be fairly well correlated by the following dimensionless equation:

$$\frac{q_{c0}}{GH_{fg}} = 8.20\left(\frac{\rho_v}{\rho_l}\right)^{0.65}\left(\frac{\sigma\rho_l}{G^2l}\right)^{0.453}\frac{1}{1+107\left(\frac{\sigma\rho_l}{G^2l}\right)^{0.54}\frac{l}{d}}. \tag{15}$$

Figure 13 shows the comparison of equation (15) with all the experimental data of q_{c0} in this regime. As it has been pointed out by Becker *et al.* [10], and as it will be clarified afterward in Section 5 of the present paper, this regime makes its appearance when the pressure is considerably high, so that this regime is called HP-regime in the present paper. It may be of interest to note here that the experimental data compiled by Thompson and Macbeth [6] includes those data belonging to HP-regime, which will be described afterward in Section 6.3.

5. BOUNDARIES OF EACH REGIME

In the existing circumstances of study, it is difficult to extend the discussion to the transition region which ought to lie between the principal regimes mentioned in Sections 3 and 4. Therefore, in the present paper, the boundary of each regime will be determined approximately by neglecting the transition region as follows.

First, by eliminating q_{c0} from equations (12) and (13), the boundary between *L*- and *H*-regime is determined as:

$$\frac{l}{d} = \frac{1}{0.4(\rho_v/\rho_l)^{0.133}(\sigma\rho_l/G^2l)^{0.29}-0.0031} \tag{16}$$

where the constant 0.4 on the RHS is to be replaced by 0.29 for Freons.

Next, for the boundary between H- and N-regime, if q_{c0} is eliminated from equations (12) and (14), it yields

$$\frac{l}{d} = \frac{1.077}{(\sigma\rho_l/G^2l)^{0.37}}, \tag{17}$$

but this does not correspond to the boundary itself as it can readily be seen in Fig. 10. Accordingly, the experimental data are classified into two groups depending on whether the linear relationship of $q_c - \Delta H_i$ holds or not, yielding the result of Fig. 14, where blank, that is non-black, symbols correspond to the experiments having the linear relationship of the type A in Fig. 4 while black symbols the non-linear relationship of the type B in Fig. 4. Then, from the slant boundary line obtained in Fig. 14, the H–N boundary is given as:

$$\frac{l}{d} = \frac{0.77}{(\sigma\rho_l/G^2l)^{0.37}}. \tag{18}$$

Finally, by eliminating q_{c0} from equations (12) and (15), the boundary between H- and HP-regime is determined as:

$$\frac{l}{d} = \frac{82(\rho_v/\rho_l)^{0.517}-(\sigma\rho_l/G^2l)^{-0.12}}{107(\sigma\rho_l/G^2l)^{0.42}-0.254(\rho_v/\rho_l)^{0.517}}. \tag{19}$$

Boundaries of each regime based on equations (16), (18), and (19) are shown with ρ_v/ρ_l as the parameter in Fig. 15, where H–L boundary lines for Freons are slightly shifted toward right due to the change of a constant in equation (16) as shown by two examples for $\rho_v/\rho_l = 0.000604$ and 0.0481. According to Fig. 15, it is noted that as ρ_v/ρ_l or the

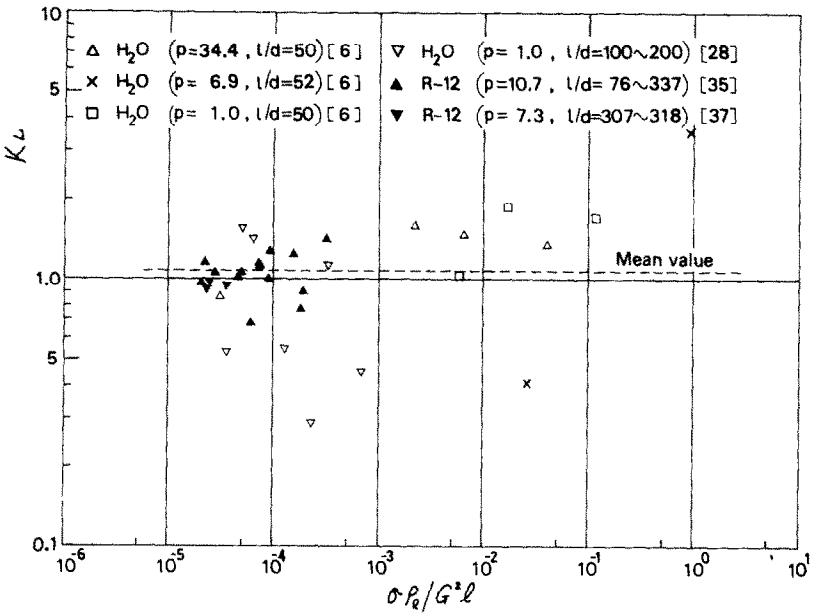

FIG. 16. Correlation of the experimental data of K_L.

pressure increases, L-regime extends to the region of lower $\sigma\rho_l/G^2l$, while H-regime extends to the region of higher $\sigma\rho_l/G^2l$. In consequence of this change, H-regime narrows and it is seen that when $\rho_v/\rho_l = 0.325$ (N.B. the corresponding pressure, 196 bar in the case of water for instance, is very near the critical pressure, 221 bar), H-regime is very narrow. On the other hand, the boundary between H- and N-regime is not affected by ρ_v/ρ_l. In addition, it should be noted that there is no transition between N- and HP-regime; that is, the transitions of H⇄N and H⇄HP alone can take place.

6. EFFECT OF INLET SUBCOOLING ON CHF

When the liquid is subcooled at the entrance of the tubes, and the linear relationship of $q_c - \Delta H_i$ (type A in Fig. 4) holds, one can write

$$q_c = q_{c0}(1 + K\Delta H_i/H_{fg}) \tag{20}$$

where K, that is a non-dimensional parameter independent of $\Delta H_i/H_{fg}$, can be determined from the gradient of the straight line A in Fig. 4.

6.1. K *in L-regime:* K_L

Figure 16 shows K_L *obtained from the data of* water and Freons belonging to L-regime (N.B. K_L cannot be obtained from the existing data of liquid nitrogen and hydrogen [38] because of the experimental range of $\Delta H_i \neq 0$). From the mechanism of CHF mentioned in Section 4.1, it may be presumed that $K_L \doteqdot 1$ for L-regime; and in fact, the mean value of all the data shown in Fig. 16 is found to be

$$K_L = 1.16 \tag{21}$$

though scattering of the value of K_L is not small as seen in Fig. 16.

6.2. K *in* H-*regime:* K_H

Figure 17 shows the correlation of K_H obtained from all the data of water and Freons belonging to H-regime, and it is formulated as follows:

$$\left.\begin{aligned} &\text{for } \sigma\rho_l/G^2l < 3\times10^{-6},\\ &\quad K_H = 1.8\left(\frac{l/d}{130}\right)^{-5\rho_v/\rho_l}\\ &\text{for } 3\times10^{-6} < \sigma\rho_l/G^2l,\\ &\quad K_H = 0.075\left(\frac{l/d}{130}\right)^{-5\rho_v/\rho_l}\left(\frac{\sigma\rho_l}{G^2l}\right)^{-1/4}. \end{aligned}\right\} \tag{22}$$

As for Fig. 17, it may be noted that in the region of small $\sigma\rho_l/G^2l$, a few exceptional data lie in the neighborhood of the broken line, but future research will be required to clarify this ambiguous phenomenon.

6.3. K *in HP-regime:* K_{HP}

Among the experimental data belonging to HP-regime, those of Chojnowski *et al.* [29] alone permit us to evaluate K_{HP} directly from the gradient of linear relation of $q_c - \Delta H_i$. The data compiled by Thompson and Macbeth (data* for $l/d = 365$ only in Tables 11–14) [6] and the data of Becker *et al.* (data of inlet subcooling 100°C in Fig. 12) [10] are composed of the independent combinations of q_c and ΔH_i. For these data, therefore, K_{HP} has been determined from equation (20) by employing the value of q_{c0} which is determined by equation (15). Figure 18 shows the correlation of K_{HP} thus obtained, and it is formulated as follows:

* It is revealed by the discrimination by means of Fig. 15 that the data for $l/d = 11.7, 50.0$, and 80.0 do not belong to HP-regime but to N-regime.

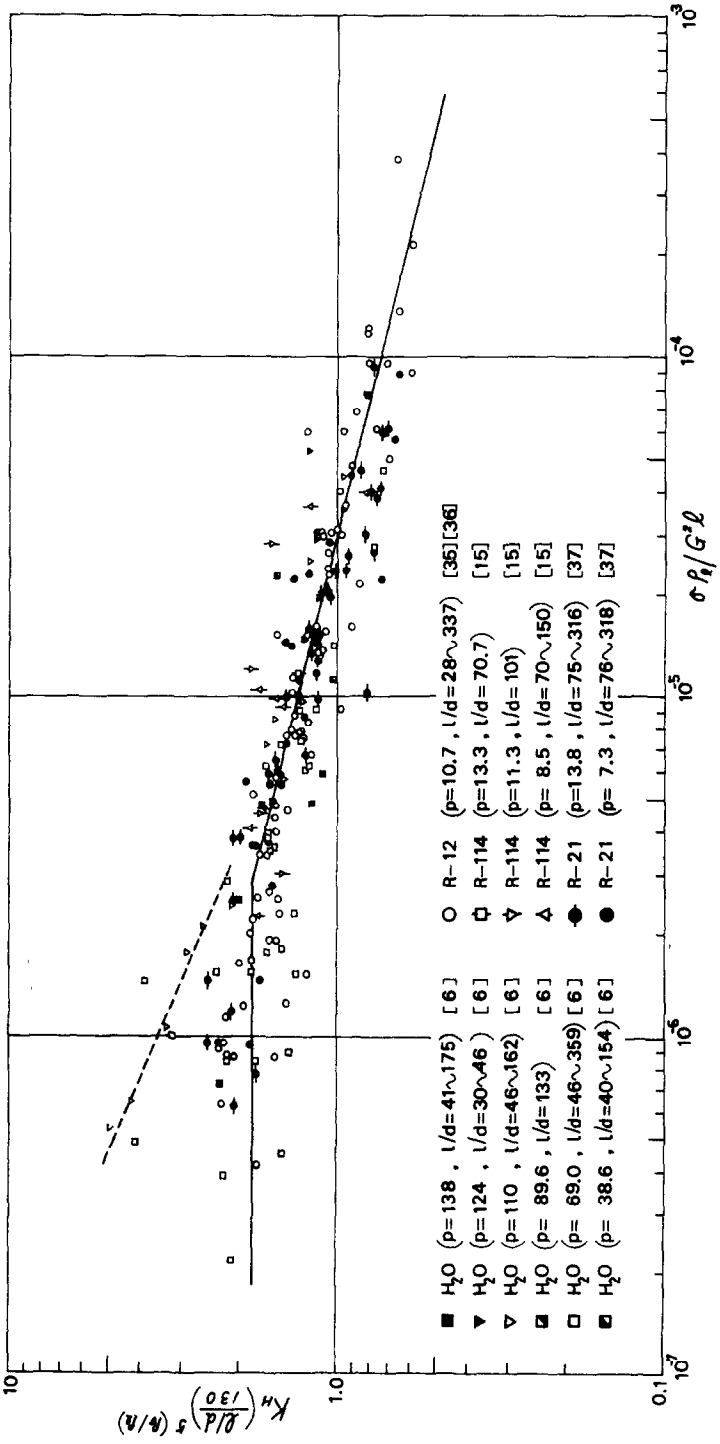

FIG. 17. Correlation of the experimental data of K_H.

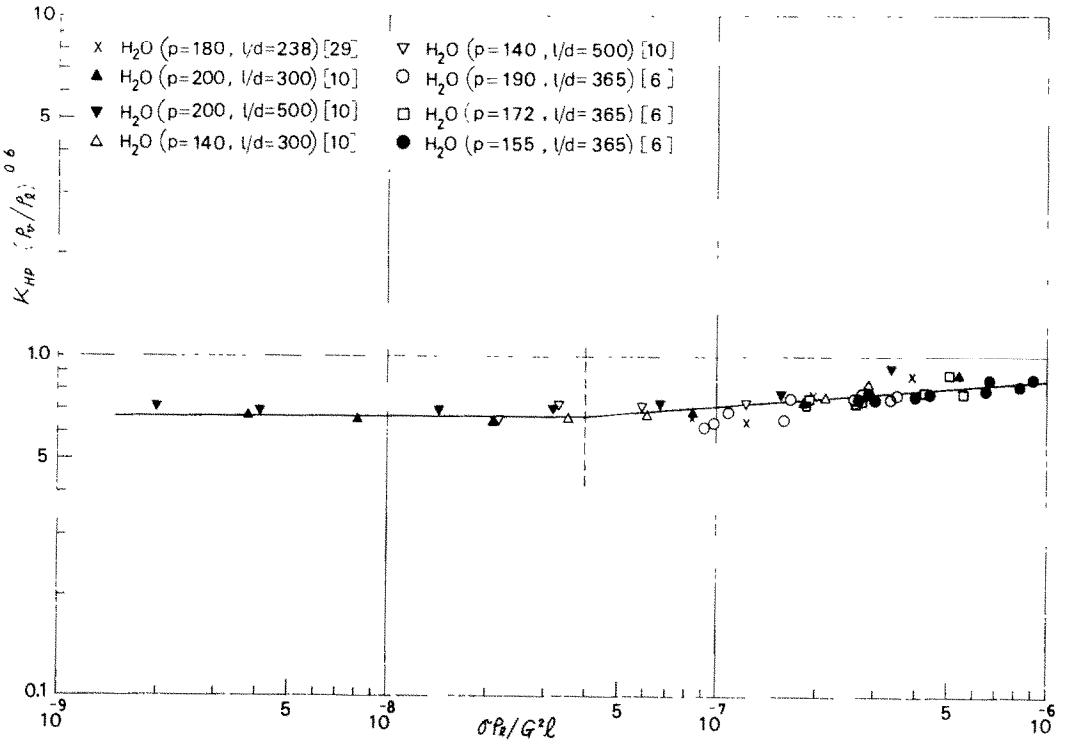

FIG. 18. Correlation of the experimental data of K_{HP}

for $\sigma\rho_l/G^2l<4\times10^{-8}$,

$$K_{HP}=0.664\,(\rho_v/\rho_l)^{-0.6}$$

for $4\times10^{-8}<\sigma\rho_l/G^2l$,

$$K_{HP}=3.08\,(\sigma\rho_l/G^2l)^{0.09}(\rho_v/\rho_l)^{-0.6}. \tag{23}$$

6.4. *Effect of inlet subcooling in N-regime*

For N-regime with the complexity of non-linear relationship for $q_c-\Delta H_i$, there is insufficient experimental data at present to produce correlations for the effect of inlet subcooling.

7. RELATION BETWEEN q_c AND χ_{ex}

For a uniformly heated tube, the heat flux q_c is related to the exit quality χ_{ex} via the heat balance, thus,

$$\frac{4q_c}{GH_{fg}}\frac{l}{d}-\frac{\Delta H_i}{H_{fg}}=\chi_{ex}. \tag{24}$$

Eliminating $\Delta H_i/H_{fg}$ from equations (20) and (24), and rearranging q_{c0} by equations (12), (13), and (15) respectively, it yields

for L-regime,

$$\frac{q_c}{GH_{fg}}=0.25\left(\frac{\sigma\rho_l}{G^2l}\right)^{0.043}\frac{K_L\chi_{ex}-1}{\left[K_L\left(\frac{\sigma\rho_l}{G^2l}\right)^{0.043}-1\right]\frac{l}{d}} \tag{25}$$

where the constant 0.25 is to be replaced by 0.34 for Freons, and K_L is given by equation (21); and

for H-regime,

$$\frac{q_c}{GH_{fg}}=0.10\left(\frac{\rho_v}{\rho_l}\right)^{0.133}\left(\frac{\sigma\rho_l}{G^2l}\right)^{1/3}\times\frac{1-K_H\chi_{ex}}{1+\left[0.0031-0.40\,K_H\left(\frac{\rho_v}{\rho_l}\right)^{0.133}\left(\frac{\sigma\rho_l}{G^2l}\right)^{1/3}\right]\frac{l}{d}} \tag{26}$$

where K_H is given by equation (22); and

for HP-regime,

$$\frac{q_c}{GH_{fg}}=8.20\left(\frac{\rho_v}{\rho_l}\right)^{0.65}\left(\frac{\sigma\rho_l}{G^2l}\right)^{0.453}\times\frac{1-K_{HP}\chi_{ex}}{1+\left[107\left(\frac{\sigma\rho_l}{G^2l}\right)^{0.54}-32.8K_{HP}\left(\frac{\rho_v}{\rho_l}\right)^{0.65}\left(\frac{\sigma\rho_l}{G^2l}\right)^{0.453}\right]\frac{l}{d}} \tag{27}$$

where K_{HP} is given by equation (23).

It should be stressed that equations (25) to (27) can apply only to the range of χ_{ex} corresponding to the possible range of $\Delta H_i/H_{fg}$ through equation (24).

8. CONCLUSIONS

Regarding CHF for the forced convection boiling in vertical uniformly heated round tubes, the experimental data of CHF for water, Freon-12, Freon-21, Freon-114, liquid nitrogen, liquid para-hydrogen and liquid herium I have been analyzed. As a result,

four regimes of CHF, called L-, H-, N-, and HP-regimes, have been classified, and employing the dimensionless groups of q_c/GH_{fg}, ρ_v/ρ_l, $\sigma\rho_l/G^2l$, l/d, and $\Delta H_i/H_{fg}$, equations (12) to (15) have been obtained for the correlation of CHF at zero inlet subcooling, Fig. 15 for the boundaries of each regime, and equations (21)–(23) for the effect of inlet subcooling on CHF.

It is hoped that through further testing against experiment, the above dimensionless correlation will be improved or modified in the future so as to predict CHF with much higher accuracy.

Acknowledgements—The author wishes to pay his respects to all the authors reporting the experimental data used in the present study. The financial support provided by the Ministry of Education is also gratefully acknowledged and the author expresses his appreciation to Prof. H. Kusuda, Dr. H. Ogata, Dr. Y. Sudoh, Mrs. M. Onami and Mr. S. Yokoya for offering the important aid which is necessary for developing this study.

REFERENCES

1. L. S. Tong, *Boiling Heat Transfer and Two Phase Flow*, p.135. John Wiley, New York (1965).
2. J. G. Collier, *Convective Boiling and Condensation*, p.236. McGraw-Hill, New York (1972).
3. W. M. Rohsenow and J. P. Hartnett (editors), *Handbook of Heat Transfer*, Section 13. McGraw-Hill, New York (1973).
4. V. Marinelli, Critical heat flux, a review of recent publications, *Nucl. Technol.* **34**, 135 (1977).
5. L. S. Tong, H. B. Currin and A. G. Thorpe II, New correlations predict DNB conditions, *Nucleonics* **21**(5), 43 (1963).
6. B. Thomson and R V. Macbeth, Boiling water heat transfer burnout in uniformly heated round tubes. a compilation of world data with accurate correlations, AEEW-R 356 (1964).
7. S. Bertoletti, G. P. Gaspari, C. Lombardi, G. Peterlongo and M Silverstri, Heat transfer crisis with steam–water mixtures, *Energia Nucl.* **12**, 121 (1965).
8. L. S. Tong, An evaluation of the departure from nucleate boiling in bundles of reactor fuel rods, *Nucl. Sci. Engng* **33**, 7. (1968).
9. G F. Hewitt, H. A Kearsy and J. G. Collier, Correlation of critical heat flux for the vertical flow of water in uniformly heated channels, AERE-R 5590 (1970).
10. K M. Becker, D Djursing, K. Lindberg, O. Eklind and C. Österdahl, Burnout conditions for round tubes at elevated pressures, *Progress in Heat and Mass Transfer*, Vol 6, p 55. Pergamon Press, Oxford (1972).
11. R. W. Bowring, A simple but accurate round tube uniform heat flux, dry-out correlation over the pressure range 0.7-12 MN/m^2 (100–2500psia), AEEW-R 759 (1972).
12. P G. Barnett, The scaling of forced convection boiling heat transfer, AEEW-R 134 (1963).
13. S Y Ahmad, Fluid to fluid modeling of critical heat flux, *Int. J. Heat Mass Transfer* **16**, 641 (1973).
14. G. F Stevens and G. J. Kirby, A quantitative comparison between data for water at 1000psia and Freon-12 at 155psia, uniformly heated round tubes, vertical upflow, AEEW-R 327 (1964).
15. G. E. Dix, Freon-water modeling of CHF in round tubes, ASME-Paper No. 70-HT-26 (1970).
16. P B. Whalley, P. Hutchinson and G. F. Hewitt, The calculation of critical heat flux in forced convection boiling, in *Heat Transfer* 1974, Vol. 4, p. 290. Hemisphere (1974).
17. E. J. Thorgerson, D. H. Knoebel and J. H. Gibbons, A model to predict convective subcooled critical heat flux, *J. Heat Transfer* **96**, 79 (1974).
18. B. Zenkevich, Similitude relations for critical heat loading in forced liquid flow, *Atomn. Energ.* **4**, 74 (1958)
19. P. Griffith, A dimensional analysis of the departure from nucleate boiling heat flux in forced convection, WAPD-TM-210 (1959).
20. J. H. Lienhard and V. K. Dhir, Hydrodynamic prediction of peak pool-boiling heat fluxes from finite bodies, *J. Heat Transfer* **95**, 152, (1973).
21. N. Zuber, Hydrodynamic aspects of boiling heat transfer, USAEC Rept. AECU-4439 (1959).
22. S. S. Kutateladze, Heat transfer in condensation and boiling, AEC-tr-3770 (1952).
23. J. H. Lienhard and R. Eichhorn, Peak boiling heat flux on cylinders in a cross flow, *Int. J. Heat Mass Transfer* **19**, 1135, (1976).
24. M. Monde and Y. Katto, Burnout in a high heat-flux boiling system with an impinging jet, *Int. J. Heat Mass Transfer* **21**, 295–305 (1978).
25. Y. Katto and K Ishii, Burnout in a high heat flux boiling system with a forced supply of liquid through a plane jet, *6th International Heat Transfer Conference*, Vol. 1, p. 435. National Research Council of Canada (1978).
26. H. Lamb, *Hydrodynamics*, p.373. Cambridge University Press, Cambridge (1932).
27. E D. Waters, J. K. Anderson, W. L. Thorne, and J. M. Batch, Experimental observations of upstream boiling burnout, A.I.Ch.E. reprint No. 7 (1963).
28. W. H. Lowdermilk, C. D. Lanzo and B. L. Siegel, Investigation of boiling burnout and flow stability for water flowing in tubes, NACA TN 4382 (1958).
29. B. Chojnowski and P. W. Wilson, Critical heat flux for large diameter steam generating tubes with circumferentially variable and uniform heating, in *Heat Transfer* 1974, Vol. 4, p. 260. Hemisphere (1974).
30. D. H. Lee and J D. Obertelli, An experimental investigation of forced convection boiling in high pressure water, Part 1, AEEW-R 213 (1963).
31. B. Matzner, Basic experimental studies of boiling fluid flow and heat transfer at elevated pressures, T.I.D. 18978 (1963)
32. R. J. Weatherhead, Nucleate boiling characteristics and the critical heat flux occurrence in sub-cooled axial-flow water systems, A.N.L. 6675 (1963).
33 P. G Barnett, The relevance of burnout in uniformly heated round tubes to burnout in non-uniformly heated reactor channels, AEEW-R 362 (1964)
34. G. F Hewitt, H. A. Kearsey, P. M. Lacey and D. J. Pulling, Burn-out and film flow in the evaporation of water in tubes, *Proc Instn Mech. Engrs* **180**(3C), 206 (1965–66)
35 G. F. Stevens, D. F. Elliot and R. W. Wood, An experimental investigation into forced convection burn-out in Freon, with reference to burn-out in water, uniformly heated round tubes with vertical up-flow, AEEW-R 321 (1964).
36. G. F. Stevens, D. F Elliot and R. W. Wood, An experimental comparison between forced convection burn-out in Freon 12 flowing vertically upwards through uniformly and non-uniformly heated round tubes, AEEW-R 426 (1965)
37. P. G. Barnett and R. W. Wood, An experimental investigation to determine the scaling laws of forced convection boiling heat transfer, Part 2, AEEW-R 443 (1965).
38. J. P. Lewis, J. H. Goddykoontz and J. F. Kline, Boiling heat transfer to liquid hydrogen and nitrogen in forced flow, NASA TN D-1314 (1962).
39. H. Ogata and S. Sato, Critical heat flux for two phase flow of helium I, *Cryogenics* **13**, 610 (1976).

UNE FORMULATION GENERALE DU FLUX THERMIQUE CRITIQUE POUR L'EBULLITION EN CONVECTION FORCEE DANS DES TUBES CIRCULAIRES, VERTICAUX ET UNIFORMEMENT CHAUFFES

Résumé—L'étude concerne le flux thermique critique (CHF) dans des conditions telles que le fluide attaquant les tubes est sous-refroidi (incluant le liquide saturé, en situation extrême) sans entrainement de vapeur. Postulant qu'il y a un état où la condition hydrodynamique est responsable du CHF, on essaie une équation de formulation générale du CHF, à l'aide de l'analyse dimensionnelle vectorielle. On analyse ensuite les résultats expérimentaux du CHF obtenus dans la bibliographie pour sept fluides différents, ce qui révèle l'existence de quatre régimes caractéristiques, désignés par régimes L, H, N et H P et conduit au développement d'une formulation générale des données de CHF aussi bien que du régime de CHF.

EINE VERALLGEMEINERTE BEZIEHUNG FÜR DIE KRITISCHE WÄRMESTROMDICHTE BEIM SIEDEN MIT ERZWUNGENER KONVEKTION IN SENKRECHTEN, GLEICHFÖRMIG BEHEIZTEN, RUNDEN ROHREN

Zusammenfassung—Die vorliegende Arbeit befaßt sich mit der kritischen Wärmestromdichte (KWSD) unter der Bedingung, daß das Fluid am Eintritt in die beheizten Rohre unterkühlt ist (eingeschlossen ist als Extremfall gesättigte Flüssigkeit), ohne daß Dampf mitgeführt wird. Zu Anfang wird unter der Voraussetzung, daß es einen Zustand gibt, bei dem die hydrodynamischen Bedingungen für die KWSD verantwortlich sind, eine theoretische Annahme für die verallgemeinerte Korrelationsgleichung für die KWSD mittels der vektoriellen Dimensionsanalyse gemacht. Dann werden experimentelle Daten für die KWSD aus der Literatur für sieben verschiedene Fluide analysiert, wobei die Existenz von vier charakteristischen Bereichen der KWSD offenbar wird, in dieser Arbeit *L*–, *H*–, *N*– und *HP*–Bereich genannt. Die Analyse führt zur Entwicklung sowohl der verallgemeinerten Korrelation von KWSD–Daten als auch der KWSD–Bereiche.

ОБОБЩЕННОЕ СООТНОШЕНИЕ ДЛЯ КРИТИЧЕСКОГО ТЕПЛОВОГО ПОТОКА ПРИ КИПЕНИИ В УСЛОВИЯХ ВЫНУЖДЕННОЙ КОНВЕКЦИИ В ВЕРТИКАЛЬНЫХ РАВНОМЕРНО НАГРЕВАЕМЫХ КРУГЛЫХ ТРУБАХ

Аннотация — В работе исследуется критический тепловой поток при подаче в нагреваемые трубы недогретой свободной от примеси пара жидкости, в том числе насыщенной жидкости, находящейся в экстремальных условиях. На основании предположения о том, что критический тепловой поток определяется гидродинамикой процесса, предпринята попытка обобщить уравнение критического теплового потока с помощью векторного анализа размерностей. Проведен анализ взятых из литературы экспериментальных данных по критическому тепловому потоку для семи различных типов жидкостей и показано наличие четырёх характерных режимов критического теплового потока, названных в данной работе режимами *L*, *H*, *N* и *HP*. Этот анализ даёт возможность обобщить данные по критическому тепловому потоку, а также получить обобщенное соотношение для режима критического теплового потока.